



Original research article

Influence of annealing temperature on In_2O_3 properties grown by an ultrasonic spray CVD process



A. Bouhdjer^a, A. Attaf^{a,*}, H. Saidi^a, Y. Benkhetta^a, M.S. Aida^b, I. Bouhaf^a, A. Rhil^a

^a Physic Laboratory of Thin Films and Applications LPCMA, University of Biskra, Algeria

^b Laboratoire de Couches Minces et Interfaces Faculté des Sciences Université de Constantine, Algeria

ARTICLE INFO

Article history:

Received 28 February 2016

Accepted 19 April 2016

Keywords:

Thin film

Ultrasonic spray

Annealing temperature

Electrical properties

ABSTRACT

This article discusses influence of the annealing temperature on the structural, optical and electrical properties of indium oxide thin films which are prepared on glass substrate heated at 150 °C by ultrasonic spray technique using indium chloride as precursor solution. The deposited samples annealed at 300 °C and 500 °C for 1 h. Structural analysis of these films suggest that the films are polycrystalline with a preferred grain orientation along the (222) plane, and the crystalline state of these films improve with the increase in the annealing temperature from 300 °C to 500 °C. The optical band gap is varied in the range of 3.64–3.73 ev. UV-vis spectroscopy show that the average transmittance is about 85% in the visible region, and the optical transmittance decrease with the increase of the annealing temperature. The electrical resistivity decreases from 80 Ω cm to $9.8 \times 10^{-3} \Omega \text{ cm}$ with the increase of the annealing temperature from 300 °C to 500 °C.

© 2016 Elsevier GmbH. All rights reserved.

1. Introduction

Transparent conducting indium oxide has attracted considerable attention on account of its good electrical and optical properties. In_2O_3 is cubic with the lattice constant of $a = 10.117 \text{ \AA}$ and space group $\text{Ia}3$ [1]. It is widely used as transparent conducting material in the optoelectronic fields, such as flat panel liquid crystal displays [2], solar cells [3], organic light emitting diodes [4]. Other applications include Schottky diodes for high power electronics and transparent thin film channel transistors, such as MISFET and MESFET.

Amorphous or crystalline indium oxide thin films can be prepared by a variety of techniques such as: spray pyrolysis [5] and hydrolysis [6], vacuum and e-beam evaporation [7,8], thermal oxidation [9], RF and DC sputtering [10]. In this work, spray pyrolysis is used to prepare In_2O_3 films because of its simplicity and low cost instrumentation with high deposition efficiency [11].

It is well known that the In_2O_3 films properties are dependent from the film deposition parameters such as deposition time [11], substrate–nozzle distance (SND) [12] substrate temperature [5,13], and doping [14]. In the present study we have studied the effect of the annealing temperature on the structural, optical and electrical properties of sprayed indium oxide.

* Corresponding author.

E-mail addresses: ab.attaf@univ-biskra.dz, ab.attaf@gmail.com (A. Attaf).

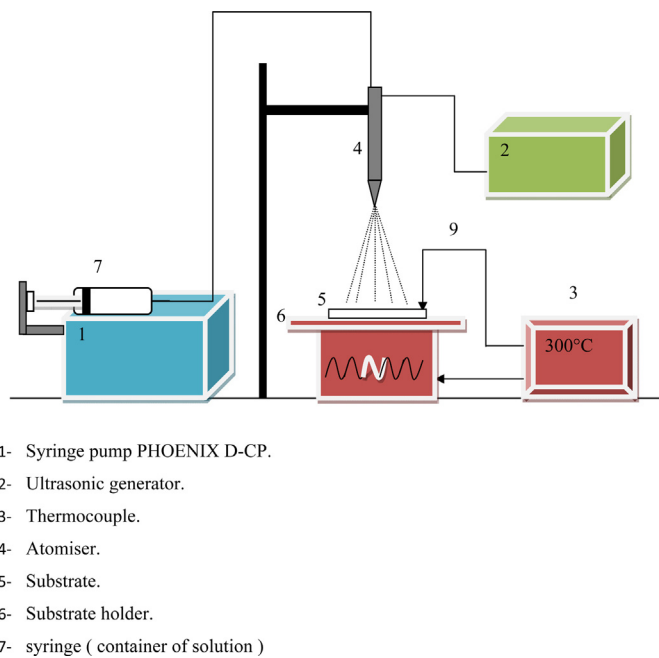


Fig. 1. Schematic diagram of the ultrasonic spray technique.

2. Experimental procedure

0.1 M of indium chloride InCl_3 (Merk, 99.9) is dissolved in methanol and sprayed onto glass substrate by ultrasonic spray technique using indium chloride as precursor solution. The schematic diagram of this setup is shown in Fig. 1. The substrate was chemically cleaned before the deposition. In the deposition process of the thin film the precursor solution was sprayed onto hot substrates ($TS = 150^\circ\text{C}$) which was at a distance of 5 cm from the spray nozzle in atmospheric pressure for 4 min as a growth time. The solution flow rate are controlled by (Syringe pump PHOENIX D-CP) and fixed at 40 ml/h. The post-deposition annealing of In_2O_3 thin films was carried out for 1 h at 300°C and 500°C in air.

The structural properties of the films were analyzed by X-ray spectroscopy on a D8 ADVANCE Diffractometer using a $\text{Cu K}\alpha$ radiation ($\lambda = 1.5405 \text{ \AA}$). The optical transmittance spectra were obtained using UV-VIS spectrophotometer, these measurements were performed using glass as reference. The electrical resistivity was determined using the four point method.

3. Results and discussion

The XRD patterns for the as-deposited In_2O_3 thin films and for the In_2O_3 films annealed at 300°C and 500°C are shown in Fig. 2. The XRD pattern of the as-deposited In_2O_3 thin film does not show any clear diffraction peak except a broad diffraction pattern for 2θ in the range of $25\text{--}35^\circ$. This indicates to the poor crystalline quality of this film and very small grain sizes in the as-deposited film. The XRD pattern obtained for the film annealed at 300°C shows reflection peaks at 30.80° and 35.66° corresponding to the (222) and (400) suggesting that film is polycrystalline in nature. However, as the annealing temperature increases to 500°C , intensity of the (222) and (400) diffraction peaks increases. This reveals the enhancement of crystallinity which is probably due to the rise in the mobility of the grains with the increase of the annealing temperature. They have also found that intensity of the diffraction peaks increased with increasing annealing temperature [15,16]. On the other hand, it is interesting to note that the XRD spectra of the film annealed at 500°C shows a shift towards lower angle for the mean peaks compared to the mean peaks of the film annealed at 300°C (see Fig. 3). This indicates a systematic lattice expansion [17,18].

Fig. 4 shows the values of FWHM for the films annealed at 300°C and 500°C . It is clear that the values of the FWHM decrease with the increase of the annealing temperature. The decreasing of FWHM values implied that the grain size increases. They have also found that average grain Size increased with increasing annealing temperature [19,20]. We believe that the increase of the grain size is based on the coalescence of small grains due to the increase in the kinetic energy of the grains by increasing the annealing temperature.

The strain (ε) values of In_2O_3 films are calculated by the following formula [21]:

$$\varepsilon = \frac{\beta \cos \theta}{4} \quad (1)$$

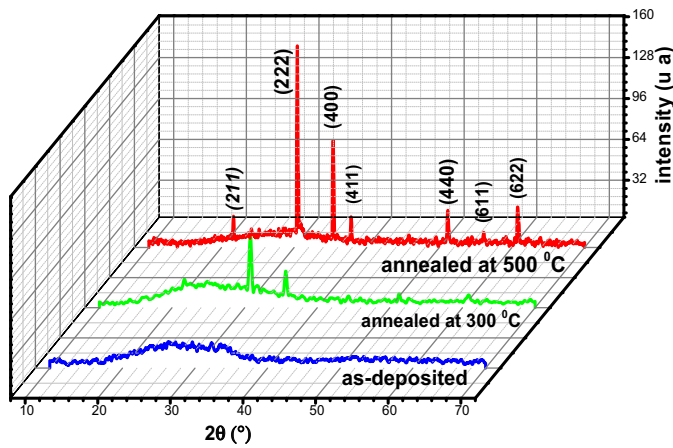


Fig. 2. XRD diffraction pattern for the as-deposited In_2O_3 thin films and for the In_2O_3 films annealed at 300 °C and 500 °C.

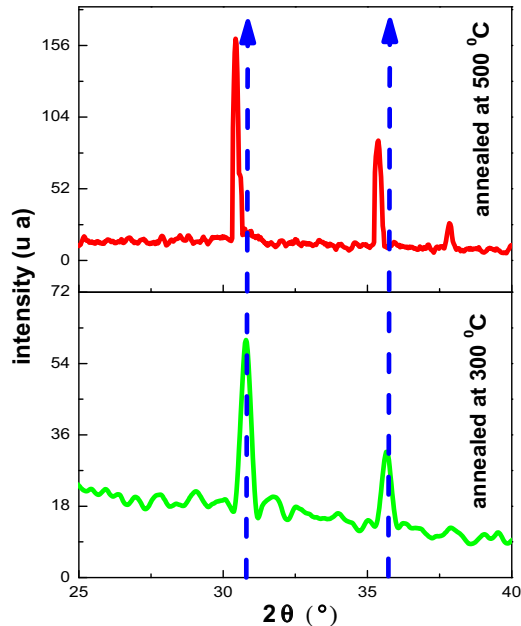


Fig. 3. Larger image for XRD diffraction pattern for the In_2O_3 films annealed at 300 °C and 500 °C.

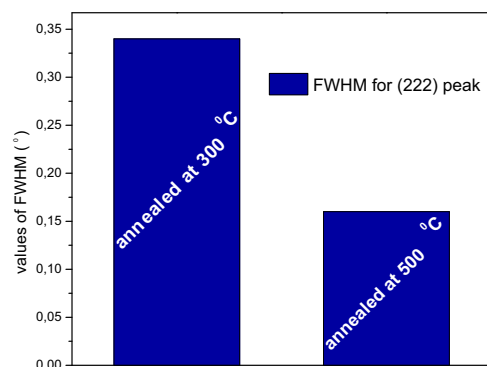


Fig. 4. FWHM for (222) peak.

Table 1

Structural parameters of In_2O_3 films at different annealing temperatures.

In_2O_3 thin film annealed at:	Lattice constant (\AA)	Dislocation density (δ) $\times 10^{14}$ lines/ m^2	strain (ε) $\times 10^{-3}$	Film thickness (nm)
300 °C	10.145	15	1.43	320
500 °C	10.088	3.01	0.6	280

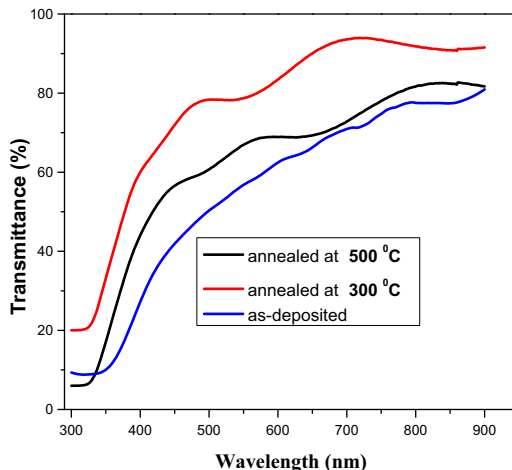


Fig. 5. Optical transmission spectra for the as-deposited In_2O_3 thin films and for the In_2O_3 films annealed at 300 °C and 500 °C.

where θ is the Bragg's angle and β is the full width at half maximum (FWHM) of the peak.

The dislocation density (δ) is calculated using the formula [22]:

$$\delta = \frac{1}{D^2} \quad (2)$$

The strain and dislocation density of (222) planes are reported in Table 1. The calculated value of lattice constant $a = 10.145 \text{\AA}$ (cubic phase) for the film annealed at 500 °C is slightly greater than the reported value 10.118\AA for pure indium oxide (JCPDS Card No. 06-0416). This can be attributed to the oxygen deficiency [23] because The In_2O_3 thin films tend toward reduction when they were annealed at high temperature [20,24]. On the other hand, the dislocation density (δ) and strain (ε) show a decreasing trend with increasing in annealing temperature. This can be attributed to recrystallization process in the polycrystalline films annealed at high temperature [25].

Fig. 5 shows the dependence of the optical transmission spectra of the investigated thin films in the wavelength region 290–900 nm as a function of annealing temperature. The as-deposited In_2O_3 thin film shows low transmittance. This is owing to poor crystalline quality of this film [11] and/or non-stoichiometric of this film; excess indium atoms due to the low deposition temperature ($T = 150$ °C). But in the case of the films annealed at 300 °C and 500 °C, we found that the optical transmittance increased due to enhancement the crystalline quality of the films. However, the film annealed at 300 °C shows the high optical transmittance despite that the film annealed at 500 °C has a high crystalline quality than the film annealed at 300 °C. This can be attributed to the oxygen deficiency in the film annealed at 500 °C [20,24]. It is well known that the oxygen deficiency in the film contributes to the blackening of the films [26,27].

The optical band gap of In_2O_3 films is estimated from Tauc relationship [28]

$$(\alpha h\nu)^2 = A(h\nu - E_g) \quad (3)$$

where α is absorption coefficient, A is the constant independent of photon energy ($h\nu$), h is the Planck constant and E_g is the optical band gap. The values of optical band gap are shown in Fig. 6. It is clear that the value of the optical band gap increase for the In_2O_3 films which annealed at 300 °C and 500 °C. This is due to the reduction of disorder in the film due to the improvement in crystalline quality of this layer [11], and the band tail width values of these films confirm this hypothesis (The band tail width for the films annealed at 350 and 550 is 0.380 ev and 0.377 ev, respectively). The low value of the optical band gap obtained for the as-deposited film ($E_g = 3.64$ ev) may be due to the poor crystalline quality of this film and The band tail width of the as-deposited films equals 0.480 ev. They have also found the same values of optical band gab [29,30].

The as-deposited film shows high electrical resistivity $100 \Omega \text{ cm}$. This is due to the poor crystalline quality of this film. Also, the film annealed at 300 °C shows high electrical resistivity $80 \Omega \text{ cm}$ although the improvement in the crystalline state of this film. This can be attributed to the excess oxygen in the film; Excess oxidation of this film for this annealing temperature [20]. The film annealed at 500 °C shows the low electrical resistivity $9.8 \times 10^{-3} \Omega \text{ cm}$. this is owing to the increase of grain size; an increase in grain size leads to reduced grain boundary scattering and thus a decrease in electrical resistivity [31].

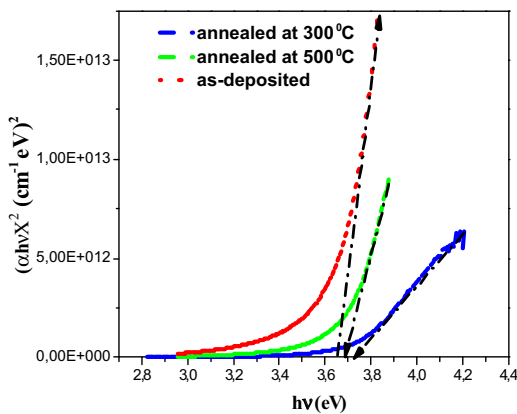


Fig. 6. Optical band gap energy for the as-deposited In_2O_3 thin films and for the In_2O_3 films annealed at 300°C and 500°C .

On the other hand, we believe that the oxygen deficiency in film due to the high annealing temperature played a role in the decrease of the electrical resistivity.

4. Conclusions

The effect of the annealing temperature on the crystalline state, optical, and electrical properties of In_2O_3 films were investigated. X-ray diffraction reveals a polycrystalline nature for all films with a preferred grain orientation along to (222). The crystalline quality of the film increase with the increase of the annealing. The dislocation density (δ) and strain (ϵ) show a decreasing trend with increasing in annealing temperature.

The optical characterization showed that our films are transparent. We have found also that the optical gap is 3.73 eV for the film annealed at 300°C and 3.69 for the film annealed at 500°C . The film annealed at 500°C showed lower value of electrical resistivity (ρ).

References

- [1] M. Morezio, Acta Crystallogr. 20 (1966) 723.
- [2] R. Latz, K. Michael, M. Scherer, Jpn. J. Appl. Phys. 30 (1991) L149.
- [3] A.S.A.C. Diniz, Renew. Energy 36 (2011) 1153.
- [4] V. Bulovic, P. Tian, P.E. Burrows, M.R. Gokhale, S.R. Forrest, M.E. Thompson, Appl. Phys. Lett. 70 (1997) 2954.
- [5] J.-H. Lee, B.-O. Park, Surf. Coat. Technol. 184 (2004) 102.
- [6] S. Kulaszewicz, Thin Solid Films 76 (1981) 89.
- [7] K.R. Murali, V. Sambasivam, M. Jayachandran, M.J. Chockalingam, N. Rangarajan, V.K. Venkatesan, Surf. Coat. Technol. 35 (1988) 297.
- [8] J.K. Sheu, Y.K. Su, G.C. Chi, M.J. Jou, C.M. Chang, Appl. Phys. Lett. 72 (1999) 3317.
- [9] M. Girtan, G.I. Rusu, Mater. Sci. Eng. B 76 (2000) 156.
- [10] A.S. Ryzhikov, R.B. Vasiliev, M.N. Rumyantseva, et al., Mater. Sci. Eng. B 96 (2002) 268.
- [11] A. Bouhdjer, et al., J. Semicond. 36 (8) (2015), 082002-1.
- [12] J. Joseph Prince, et al., J. Cryst. Growth 240 (2002) 142–151.
- [13] M. Girtan, Surf. Coat. Technol. 184 (2004) 219–224.
- [14] S. Parthiban, E. Elangovan, K. Ramamurthi, R. Martins, E. Fortunato, Sol. Energy Mater. Sol. Cells 94 (2010) 406–412.
- [15] A. Sudha, S.L. Sharma, T.K. Maity, Mater. Lett. 157 (2015) 19–22.
- [16] J.-H. Cha, K. Ashok, N.J.S. Kissinger, J Korean Phys. Soc. 3 (September (3)) (2011) 2280–2285.
- [17] D. Mergel, W. Stass, G. Ehl, D. Barthel, J. Appl. Phys. 88 (2000) 2437.
- [18] Z. Qiao, R. Latz, D. Mergel, Thin Solid Films 466 (2004) 250–258.
- [19] S. Cho, Microelectron. Eng. 89 (2012) 84–88.
- [20] Kazuhiro Kato, Hideo Omoto, Takao Tomioka, Thin Solid Films 520 (2011) 110–116.
- [21] K.L. Chopra, Thin Film Phenomena, McGraw-Hill, New York, 1969, pp. 270.
- [22] J.I. Pankove, Optical processes in semiconductors, Dover, New York, 1975.
- [23] N.G. Pramod, S.N. Pandey, P.P. Sahay, Ceram. Int. 38 (2012) 4151–4158.
- [24] D.R. Gaskell, Introduction to the Thermodynamics of Materials, 4th ed., Taylor & Francis, 2009.
- [25] A. Moses EzhilRaja, K.C. Lalithambika, Phys. B 403 (2007) 544.
- [26] W.F. Wu, B.S. Chiou, Thin Solid Films 247 (1994) 201.
- [27] W.F. Wu, B.S. Chiou, Semicond. Sci. Technol. 11 (1996) 196.
- [28] J. Bardeen, F.J. Blatt, L.H. Hall, Proceedings of Atlantic City Photoconductivity Conference in 1954, Wiley and Chapman and Hall, New York, 1956, p. 146.
- [29] M. Jothibas, et al., J. Mol. Struct. 1049 (2013) 239–249.
- [30] N.G. Pramod, S.N. Pandey, Ceram. Int. 40 (2014) 3461–3468.
- [31] H. Kim, J.S. Horwitz, G.P. Kushto, S.B. Qadri, Z.H. Kafafi, D.B. Chrisey, Appl. Phys. Lett. 78 (2001) 1050.